

Integrating Feature Selection and Machine Learning for Nitrogen Assessment in Grapevine Leaves using In-Field Hyperspectral Imaging

Atif Bilal Asad^{a,1,*}, Achyut Paudel^a, Safal Kshetri^a, Chenchen Kang^c, Salik Ram Khanal^d, Nataliya Shcherbatyuk^e, Pierre Davadant^h, R. Paul Schreiner^{f,2}, Santosh Kalauni^g, Manoj Karkee^b, Markus Keller^e

^a*Center for Precision and Automated Agricultural Systems, Washington State University, Prosser, 99350, WA, USA*

^b*Biological & Environmental Engineering Department, Cornell University, Ithaca, 14853, NY, USA*

^c*Fruit Research and Extension Center, The Penn State University, Biglerville, 17307, PA, USA*

^d*School of Business and Technology, Curry College, Milton, 02186, MA, USA*

^e*Department of Viticulture and Enology, Washington State University, Prosser, 99350, WA, USA*

^f*USDA-ARS, Horticultural Crops Production and Genetic Improvement Research Unit (HCPGIRU), Corvallis, 97330, OR, USA*

^g*Mid-Columbia Agricultural Research and Extension Center, Oregon State University, Corvallis, 97031, OR, USA*

^h*Department of Plant Sciences, University of Tennessee, Institute of Agriculture, Knoxville, 37996, TN, USA*

Abstract

Nitrogen (N) is one of the most crucial nutrients in vineyards, affecting plant growth and subsequent products such as wine and juice. Because soil N has high spatial and temporal variability, it is desirable to accurately estimate the N concentration of grapevine leaves and manage fertilization at the individual plant level to optimally meet plant needs. In this study, we used in-field hyperspectral images with wavelengths ranging from 400to1000nm of four different grapevine cultivars collected from distinct vineyards and over two growth stages during two growing seasons to develop models for predicting N concentration at the leaf-level and canopy-level. After image processing, two feature selection methods were employed to identify the optimal set of spectral bands that were responsive to leaf N concentrations. The selected spectral bands were used to train and test two different Machine Learning (ML) models, Gradient Boosting and XGBoost, for predicting nitrogen concentrations. The comparison of selected bands for both leaf-level and canopy-level datasets showed that most of the spectral regions identified by the feature selection methods were across both methods

and the dataset types (leaf- and canopy-level datasets), particularly in the key regions, 500 – 525nm, 650 – 690nm, 750 – 800nm, and 900 – 950nm. These findings indicated the robustness of these spectral regions for predicting nitrogen content. The results for N prediction demonstrated that the ML model achieved an R^2 of 0.49 for canopy-level data and an R^2 of 0.57 for leaf-level data, despite using different sets of selected spectral bands for each analysis level. The study demonstrated the potential of using in-field hyperspectral imaging and the use of spectral data in integrated feature selection and ML techniques to monitor N status in vineyards.

Keywords: In-field hyperspectral imaging, Grapevine, Leaf-level, PLSR, Ensemble, Nitrogen, Vitis

1. Introduction

Grape cultivation is a key part of the global agriculture industry. It supports millions of jobs—from vineyard management to winemaking and export logistics, and significantly contributes to economies worldwide, including the U.S. The overall grape production in the U.S. is valued at over \$6.8 billion, making it one of the highest-value fruit crops in the country. The industry includes more than 360,000 hectares of planted grapes, producing more than 5.36 million metric tons in 2023 (USDA, NASS, 2024). The profitability of grape cultivation is linked with the effective management of mineral nutrients in vineyards. Nitrogen (N) is critical for grapevine physiological processes, influencing growth, productivity, and fruit quality parameters such as sugar content, acidity, phenolics and aromatic compounds (Keller, 2020). Achieving a balance is critical, as excessive and insufficient nitrogen availability can adversely affect grape yield and quality. Abundant availability of N promotes higher canopy growth, resulting in shading of the fruit (Smart, 1991), which delays fruit ripening and causes poor fruit color development (Keller and Hrazdina, 1998). In addition, excess N

*Corresponding author: Atif Bilal Asad, Email: aba89@cornell.edu

¹Current affiliation: Biological & Environmental Engineering Department, Cornell University, Ithaca, NY, USA.

²Retired, Present address: 1414 Cedar Street, Philomath, OR 97370

resulting overfertilization remains unused in the soil, which increases the chances of nitrate (NO_3) accumulation in natural water bodies if the excess N leaches below the root zone or is lost by run-off (Jaynes et al., 2001). On the other hand, N deficiency can decrease crop yields due to reduced fruit set and berry size, while decreasing yeast assimilable nitrogen (YAN) in the juice (Schreiner et al., 2013), and increasing vulnerability to stress and disease (Thomidis et al., 2016).

Therefore, efficient N management in vineyards requires an accurate assessment of the vine's N status (Verdenal et al., 2021). Traditionally, assessing N status in grapevines is based on laborious and time-consuming methods of manually collecting and analyzing leaf tissues through laboratory chemical analysis (Robinson, 2005). This labor-intensive process of collecting field samples and conducting subsequent laboratory tests poses a significant obstacle to efficiently monitoring large-scale vineyards. Due to these limitations, current methods of assessing N in vineyards cannot offer the spatial resolution required to represent the variability of N levels within a vineyard, especially for understanding and managing the needs for N in individual vines. Furthermore, there is a time lag between sampling and when the results are available, which hampers real-time monitoring and prompt decision-making.

Recent improvements in remote sensing technologies, including hyperspectral and multispectral imaging and ML modeling, provide alternatives for assessing plant nutrient status in a non-destructive and rapid manner with high spatial resolution (Paudel et al., 2025; Chancia et al., 2021). Example studies with these technologies used the spectral signatures of plants in the visible and near-infrared regions of the electromagnetic spectrum to identify and estimate plant characteristics associated with nutrient levels in corn (Fan et al., 2019), wheat (Vigneau et al., 2011), barley (Xu et al., 2014), potato (Liu et al., 2021) and grapevines (Peanusaha et al., 2024; Chancia et al., 2021; Moghimi et al., 2018).

Specifically, hyperspectral imaging (HSI) has emerged as a promising nondestructive technique for assessing plant nutrient status. HSI facilitates the acquisition of high-resolution spectral information across a wide range of wavelengths, spanning from visible to near-infrared and shortwave infrared regions of the electromagnetic spectrum (Gowen et al., 2007). This high-dimensional spectral data enables detailed characterization of biochemical

and physiological properties of plant tissues, as various constituents exhibit unique spectral signatures (Kalacska et al., 2015). When coupled with advanced ML algorithms, HSI imaging shows excellent potential for accurately assessing grapevine N levels (Chancia et al., 2021). HSI-based studies employed various methodologies to estimate N concentration using various ML models. Among these models, some incorporated the entire spectrum range of the sensor. In contrast, others analyzed derivatives of the spectral data (Debnath et al., 2021; Lyu et al., 2023), and several vegetation indexes (Peanusaha et al., 2024), while other models used spectral transformation techniques (Chancia et al., 2021). Some modeling techniques have also used combinations of datasets mentioned above. Specific ML techniques that have been found effective to analyze these complex datasets to determine N levels in plants include support vector machines (SVM) (Yao et al., 2015), random forest regression (RFR) (Pullanagari et al., 2016), extreme learning machine (ELM) (Peng et al., 2022), and partial least squares regression (PLSR) (Chancia et al., 2021; Peanusaha et al., 2024). These ML approaches can learn complex non-linear relationships between the high-dimensional spectral data and corresponding N concentrations, enabling the development of predictive models that can be applied for rapid and non-invasive N monitoring.

Unlike multispectral sensors that capture reflectance in a few broad wavelengths, hyperspectral sensors acquire dense spectral information across hundreds of narrow wavelength bands. However, image acquisition in a large number of narrow spectral bands leads to high dimensionality of hyperspectral data, which poses significant challenges to handling huge data volumes during processing, including the need for large memory and computational resources (Adao et al., 2017), as well as the potential of data redundancy (Bioucas-Dias et al., 2013). Specifically, within a large amount of spectral data, only specific wavelengths may have a direct relevance/sensitivity to the target variable, such as varying N status. The rest of the spectral bands may be redundant or irrelevant, which makes interpretation more difficult and increases the likelihood of overfitting the prediction models to specific datasets used in the training process (Moghimi et al., 2018). Another challenge in training ML models with hyperspectral images is the limited availability of data samples, which limits the accuracy and generalizability of the ML models used. It was found that the performance

of ML models deteriorates as the number of spectral bands (features) increases while the number of training samples remains fixed. This phenomenon, known as the Hughes effect, leads to a loss of accuracy of the ML model because the model becomes overfitted to the limited dataset used in training the model (Ma et al., 2013). To mitigate these challenges and exploit the rich information provided by the hyperspectral data, researchers have explored dimension reduction techniques, such as feature selection methods, to identify the most informative spectral bands for accurate and efficient prediction of plant traits and input status (Dong et al., 2017; Rivera-Caicedo et al., 2017).

Recognizing the challenges posed by the large data volume and the many redundant features in hyperspectral imaging, our research focused on developing a feature selection pipeline that identifies the most informative set of spectral features for N assessment in grape leaves. Applying ensemble feature selection and PLSR filtering techniques, we could identify specific spectral features that strongly correlate with N concentrations in grapevine leaves—features that are typically not included in standard multispectral sensors. Our comprehensive dataset covered four different grape cultivars across two growing seasons (2022 and 2023) and two distinct geographic locations (Washington and Oregon) within the United States. This diversity helped to ensure the robustness and wide applicability of our N prediction model under real-world vineyard scenarios. The primary objectives of this study were to:

- Develop a feature selection method to identify the optimal set of features for nitrogen assessment in grapevine leaves.
- Develop models that use the optimal set of features to estimate nitrogen concentration in grapevine leaves.
- Compare and assess the effectiveness of the feature selection methods for nitrogen estimation at both leaf and canopy levels.

The results of this work enable rapid and non-destructive assessment of N in vineyards and provide information of N at the plant level. Such precise data supports the implementation of improved fertilization strategies, such as variable rate N application, ensuring that

each plant receives the optimal amount of N based on its current needs. Our work potentially provides guidance for the development of customized multispectral sensors, specifically for N assessment in plant leaves. Such sensors will indicate N status without the high computational overhead associated with complete hyperspectral data.

2. Materials and Methods

2.1. Data Collection

Spectral data and corresponding ground truth measurements of nitrogen content (based on tissue sampling) were gathered during two phenological stages of grapevine growth, bloom and veraison (i.e., onset of fruit ripening), over two growing seasons of 2022 and 2023. Four grapevine cultivars were used to collect the data listed in Table 1. This multi-year, multi-cultivar approach facilitated a comprehensive analysis of varying growth stages and environmental conditions.

Table 1: Field data collection efforts over two growing seasons. A tick (✓) indicates successful data collection for the given growth stage; a cross (×) indicates missing data. Total samples per year are shown in the last two columns, where leaf-level counts refer to the number of leaves and canopy-level counts refer to the number of grapevines.

Cultivar	Leaf/Canopy Level	2022		2023		Total Samples	
		Bloom	Veraison	Bloom	Veraison	2022	2023
Chardonnay	Leaf	✓	✓	✓	✓	132	106
Pinot Noir	Leaf	✓	✓	✓	✓	161	110
Chardonnay	Canopy	✓	✓	✓	✓	118	109
Syrah	Canopy	×	✓	✓	✓	97	137
Concord	Canopy	✓	✓	✓	✓	75	54

2.1.1. Leaf Level Spectral and Nutrient Data

This study was conducted in two commercial vineyard blocks located in Oregon, USA; *Vitis vinifera* L. cv. Pinot Noir vineyard (44°53'16" N; 122°51'06" W) and Chardonnay

vineyard ($46^{\circ}17'49''$ N; $119^{\circ}44'07''$ W). The vines were selected randomly from each vineyard for data collection, ensuring a diverse sampling. From each data vine, two leaves, well-exposed to the sun, healthy, fully developed, and proximal to the grape clusters on the same side of the canopy, were tagged for sampling. For the spectral data acquisition, we employed a VNIR hyperspectral camera (Nano-Hyperspec[®], Headwall Photonics, Bolton, MA, USA) mounted on a ground-based tripod. This setup allowed precise positioning of the camera—approximately 2 meters from the target vine and 1 meter above the ground for optimal focus on the middle of the vine’s vertical canopy. The camera’s line scanning capability covered a spectral range from 400 to 1000nm across 274 spectral bands. The operational parameters of the camera were tuned to capture high-resolution images ($\sim 3200 \times 640$ pixels). The exposure times were managed between 9 and 15 milliseconds to maintain above 90% saturation level, focusing on a white reference to ensure consistent image quality. Concurrently, the imaging frame period was synchronized with the exposure time, facilitating the determination of the scanning rate. The angular scanning speed, which varied between 1.20 and $1.85^{\circ}/\text{s}$, was calculated by using the FOV Calculator from HyperSpec III software, developed by Headwall Photonics (Kang et al., 2023). Each image acquired by the camera included both tagged leaves within the field of view, as well as both white and dark reference surfaces for calibration. Following the imaging of each vine, the leaf blades were carefully removed from the vines and individually sealed in paper bags, then transported to the laboratory for subsequent nutrient analysis. A total of 509 leaf samples from 255 data vines were used for this data collection.

2.1.2. Canopy Level Spectral and Nutrient Data

This data collection was conducted with three grapevine cultivars located in Washington, USA, two commercial wine grape blocks at Columbia Crest Winery ($45^{\circ}57'25.95''$ N, $119^{\circ}36'34.41''$ W) of *V. vinifera* cv. Chardonnay and Syrah and a block ($46^{\circ}19'4.84''$ N, $119^{\circ}55'56.51''$ W) of Concord, a juice grape hybrid cultivar with *Vitis labrusca* L. and *V. vinifera* ancestry. To maintain uniformity in data collection, the selected data vines were consistently sampled at both growth stages and both growing seasons listed in Table 1. The

image acquisition process was carried out exactly as described in 2.1.1. Tissue sampling, however, was conducted differently. For this canopy-level study, each sample contained 20 to 40 completely developed leaves carefully removed from each data vine near the grape clusters. To maintain the biochemical integrity of the gathered leaves, they were sealed in a plastic bag before being sent to a commercial laboratory (Soiltest Farm Consultants, Moses Lake, WA, USA) for nutrient analysis. The total number of samples for this dataset was 591 from 200 data vines.

2.2. Data Analysis

2.2.1. Spectral Data Preparation - Leaf Level

At the leaf level, the N concentration was measured from individual leaves by combustion analysis and conversion to N_2 using the Dumas method using a C-H-N Analyzer, and the corresponding spectral data was extracted for each leaf. In contrast, canopy-level processing aggregates spectral data from several leaves (typically 10–20 per vine) to produce a composite measurement representing the overall canopy, which offers a broad view of the vine’s nutrient status, discussed in section 2.2.2. The process of extracting leaf-level spectral data consisted of reflectance correction, leaf segmentation, and reflectance spectra extraction from individual leaf areas. First, reflection correction on the spectral data was performed using Eq. 1:

$$I_{c(i,j,\lambda)} = \frac{I_r(i,j,\lambda) - I_{\text{dark}(i,j,\lambda)}}{I_{\text{white}(i,j,\lambda)} - I_{\text{dark}(i,j,\lambda)}} \times (\text{Absolute reflectance of White Reference}) \quad (1)$$

where, I_c is the corrected reflectance of a given pixel, I_r is the intensity of light at the pixel; i and j are the spatial coordinates of the pixel, λ is the wavelength; and I_{white} , I_{dark} are the white and dark references (Kang et al., 2023). The absolute reflectance of white reference is the known standardized reflectance value of a white reference material (often close to 1, or 100 % reflectance) under ideal conditions. In Eq. 1, the term $(I_r - I_{\text{dark}})/(I_{\text{white}} - I_{\text{dark}})$ calculates the relative reflectance of the target compared to the white reference under the same lighting conditions; multiplying this relative reflectance by the "Absolute reflectance

of White Reference” converts this relative measurement into an absolute reflectance value of the target pixel I_c . The RGB images were generated using the wavelength bands 487.642



Figure 1: Sample leaves used in the study were labeled using white tags (top); binary masks of the tagged leaves were created (middle), which were then used to extract the sample leaf areas (bottom) and extract the leaf area.

nm (B), 547.321 nm (G), and 677.732 nm (R) to facilitate accurate segmentation of the leaf area from the hyperspectral data. These bands were chosen through trial and error as they provided a good visual representation that aids in identifying the tagged leaf. After reflectance correction, the leaves were manually segmented to accurately delineate the complex canopy structure, which was chosen because of the challenge due to the similarity in color and texture between the leaves and background, as shown in Figure 1. The spectral data of all pixels within each leaf area were then averaged to obtain a single observation that represents the sample leaf.

2.2.2. Spectral Data Preparation - Canopy Level

At the canopy level, measurements were made to capture the overall N status of entire vine canopies rather than focusing on individual leaves. This approach is essential because

chemical analysis of tissue samples by commercial testing laboratories is typically performed on a composite sample—obtained by mixing 20 to 40 leaves from a single vine—which represents the average nutrient content across the entire canopy. To replicate this composite measurement approach using spectral data, after performing the spectral correction procedure outlined in Section 2.2.1, we selected 5 to 15 leaves from one side of the canopy that was fully grown and sun-exposed from each sample vine.

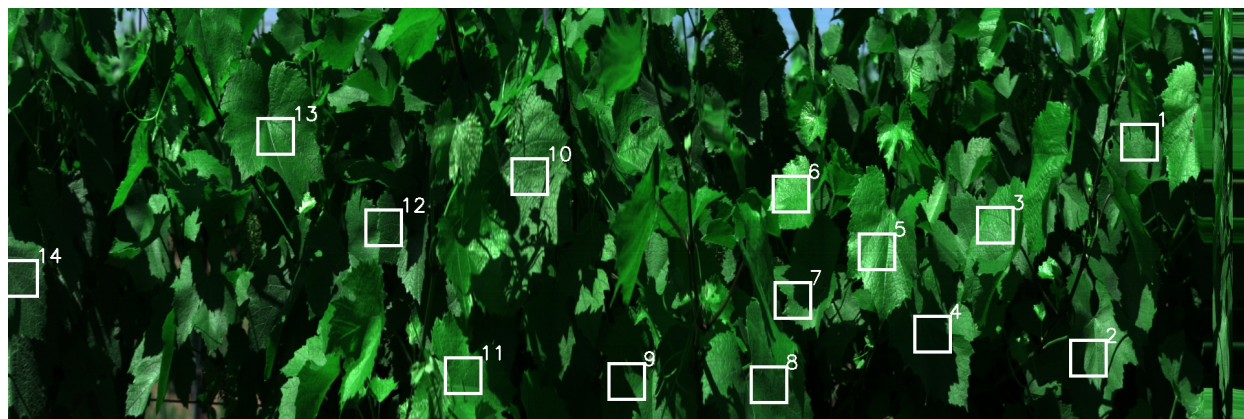


Figure 2: RGB visualization of grapevine canopy with selected 50×50 pixel regions of interest (ROIs) marked by white squares. The image was created using hyperspectral bands at 487.642 nm (blue), 547.321 nm (green), and 677.732 nm (red). Each ROI represents an area used for extracting reflectance spectra from individual leaves within the canopy.

For each selected leaf, a 50×50 -pixel bounding box was used to define the region of interest (ROI) as shown in Figure 2. The reflectance spectra were then extracted for all pixels within these ROIs and averaged to generate one representative spectral observation per vine, corresponding to the N concentration obtained from the chemical analysis at the canopy level. This canopy-level processing ensures that the spectral data reflects the integrated N concentration of the entire vine canopies, facilitating a more appropriate comparison with laboratory measurements.

2.2.3. Pre-Treatment of Spectral Data

It was observed that the first 10 and last 2 bands of the hyperspectral images exhibited significant distortions, likely due to sensor noise or edge effects inherent to the spectral

acquisition process. These distortions can lead to inaccuracies in subsequent analysis, such as feature selection and regression modeling. To ensure the integrity and reliability of the analysis, these spectral bands were excluded from the dataset. This pre-processing method was employed to process all spectral data, which included the application of standard normal variate (SNV) and Savitzky-Golay (SG) filter for smoothing. The optimal window length for the SG filter was determined using both signal-to-noise ratio (SNR) considerations and Fourier-transform frequency analysis (Chancia et al., 2021). This comprehensive approach ensured the selection of a window length that effectively reduced noise while preserving important spectral features.

2.2.4. Redundant Feature Removal

The high dimensionality often results in significant redundancy among the spectral bands, which can complicate the feature selection process, increase computational demands, and potentially lead to model overfitting. To improve the efficiency and effectiveness of the feature selection process, redundant spectral bands were removed from the dataset using hierarchical clustering. The correlation matrix of the spectral bands was calculated to understand the relationships between different spectral bands. The correlation matrix was then transformed into a distance matrix by computing $1 - \text{absolute}(\text{correlation})$, where highly correlated features (correlation coefficient close to 1) would have a distance close to 0, indicating redundancy. Then, hierarchical clustering was performed on the distance matrix using the complete linkage clustering method. In the complete linkage clustering method, the distance between two clusters is the maximum distance between any pair of features in the clusters. This means that clusters are merged only when all their members are relatively similar, resulting in compact and well-separated groups (Sharma et al., 2019). In this study, a distance threshold of 0.08 was used for both canopy-level and leaf-level data analysis. To select a representative feature from each cluster, the correlation of each feature with the target variable, measured N concentration, was calculated. Within each cluster, the feature with the highest correlation to the target variable was chosen as the cluster representative. By removing redundant features, the dimensionality of the dataset

was significantly reduced. This approach not only improved computational efficiency but also ensured that the remaining features were responsive to predicting N concentration in grapevine leaves. The streamlined dataset was subsequently used in two feature selection techniques to further refine the predictive model.

2.2.5. Ensemble Feature Selection Method

An ensemble feature selection technique was utilized to identify the most significant spectral features for predicting N concentration in grapevine leaves. To introduce variability and prevent overfitting, a dynamic data splitting approach was employed, where the dataset was repeatedly split into training and validation subsets, using 90% of the data for training in each iteration. This process was repeated 50 times with different random seeds to ensure diverse subsets (Chancia et al., 2021). Several feature selection methods were used, including SelectKBest, Lasso Regression, Ridge Regression, Random Forest Regressor, Extra Trees Regressor, and Gradient Boosting Regressor (Omidi et al., 2020). For each iteration and method, feature importances were calculated and normalized using a MinMaxScaler and converted to ranks. The ranks from all methods and iterations were aggregated to obtain an average rank for each feature, ensuring robust identification of important variables. The features were then sorted based on their average ranks, and the top-ranked features were identified as the most relevant for predicting nitrogen content. To determine the optimal number of features, a multiple linear regression model was employed using the selected features. Leave-One-Out cross-validation (LOOCV) was used to evaluate the model performance. The number of selected features was varied iteratively by adding one feature at a time based on their ranking. For each set of selected features, the model was evaluated using Root Mean Squared Error (RMSE) and the coefficient of determination (R^2). The total number of features from which adding more features did not significantly increase the model performance was determined to be the optimal set of features. This approach ensured that the selected features were not only robustly identified but also optimally selected for maximum predictive accuracy.

2.2.6. Partial Least Squares Regression (PLSR)

The systematic approach of feature selection using PLSR has been demonstrated to be effective in previous studies (Mehmood et al., 2012). In this study, PLSR was employed as a filter method for feature selection. This feature selection method consists of two steps; first, the PLSR model was fitted to the dataset using an optimal number of components to obtain relevancy measures, such as absolute regression coefficients. The absolute values of the PLS coefficients were used to rank the spectral features in terms of their importance. This ranking provided a preliminary indication of which wavelengths were most relevant for predicting N concentration in grapevine leaves. In the second step, an iterative process was employed to further refine the feature selection. Starting with the full set of ranked features, the least relevant features, as determined by the relevancy measures, were systematically excluded. The PLSR model was then recalibrated using the remaining features. This process of exclusion and recalibration continued iteratively to minimize the cross-validation mean squared error (MSE). The iterative exclusion process ensures that only the most responsive variables are retained, enhancing the model’s performance while maintaining computational efficiency.

2.2.7. Model Development and Evaluation

As discussed before, two feature selection methods, PLSR and Ensemble Feature Selection, were employed to identify significant spectral features using both the leaf-level dataset and the canopy-level dataset. Each method was independently applied to both datasets. The features that were common to both datasets were identified. These common features and their corresponding reflectance values were then used to predict N concentration. In this study, two machine learning models—XGBoost and Gradient Boosting—were employed to predict N concentration from the selected features. These models are powerful ensemble methods that are effective at capturing non-linear relationships and feature interactions, which are essential when working with spectral data (Zou et al., 2025; Liu et al., 2017). XGBoost is renowned for its efficiency and built-in regularization that helps prevent overfitting, while Gradient Boosting provides a robust alternative through its sequential learning

approach. To optimize the machine learning models, we used GridSearchCV for hyperparameter tuning.

Table 2: Hyperparameter ranges for XGBoost and Gradient Boosting models used for N prediction in grapevine leaves.

Model	Hyperparameter	Values Explored
XGBoost	Number of Estimators	100, 500, 1000
	Maximum Depth	3, 5, 7, 10
	Learning Rate	0.01, 0.05, 0.1
	Subsample	0.5, 0.7, 1.0
Gradient Boosting	Number of Estimators	100, 200
	Maximum Depth	3, 5
	Learning Rate	0.01, 0.1
	Subsample	0.5, 0.7

GridSearchCV systematically evaluates all combinations of hyperparameters from a pre-defined range, Table 2, using 10-fold cross-validation to assess each setting. In this process, the data was partitioned into training and validation sets; models were trained on 90% of the data and validated on the remaining 10%, with this process repeated 10 times to ensure robustness and mitigate overfitting. Model performance was evaluated using three metrics: R^2 , RMSE, and MAE, using the 10-fold cross-validation strategy. We compared the performance of the two ML models to determine which model better predicts N using the selected features. Furthermore, we compared results from the leaf-level and canopy-level datasets to assess how the scale of spectral data impacts prediction accuracy. This comprehensive comparison allowed us to determine the optimal model and data resolution for N estimation, ensuring that the chosen approach is both accurate and robust for practical vineyard management applications.

All data processing methods and techniques were implemented using Python 3.6, unless specified otherwise,

3. Results and Discussions

3.1. Nitrogen level of the sample vines

Table 3 presents a summary of N concentrations of the grapevine leaves measured using chemical analysis. The N concentration exhibited significant variability among different cultivars and seasons, as shown in Figure 3. In the leaf-level dataset, the N concentration of both Chardonnay and Pinot Noir cultivars typically varied from 0.99% to 3.43% dry weight (DW) of grapevine leaves. In contrast, the canopy-level N data include three cultivars, Chardonnay, Syrah, and Concord, which have N concentration primarily ranging from 2.36% to 3.72% DW of leaf blades, with a mean value of approximately 2.9% DW. The histograms demonstrate the variations in N concentration in grapevine leaves throughout two growing seasons, highlighting the impact of both cultivar type and phenological stage on leaf N concentration.

Table 3: Descriptive statistics of nitrogen (N) concentration per unit dry weight (DW) of grapevine leaves, summarized by cultivar and measurement level.

Measurement Level	Cultivar	Min–Max (% DW)	Mean (% DW)	STD (% DW)
Leaf Level	Pinot Noir	1.63–3.43	2.36	0.35
	Chardonnay	0.99–3.22	2.10	0.45
Canopy Level	Chardonnay	2.38–3.70	2.92	0.28
	Syrah	2.36–3.72	3.03	0.29
	Concord	2.50–3.72	3.11	0.24

From the histogram, it was observed that the N concentration was consistently higher during bloom (peak to the right) and decreased by veraison (peak to the left) across all cultivars except Chardonnay in 2022, as shown in Figure 3. This difference largely reflects the change in leaf age during the growing season: N concentrations are typically high in young tissues and decrease along with chlorophyll content as leaves age (Keller, 2020; Verdenal et al., 2021).

It was also observed that canopy-level samples displayed a narrower range of N concentrations but higher mean values compared to leaf-level samples. This variation is largely

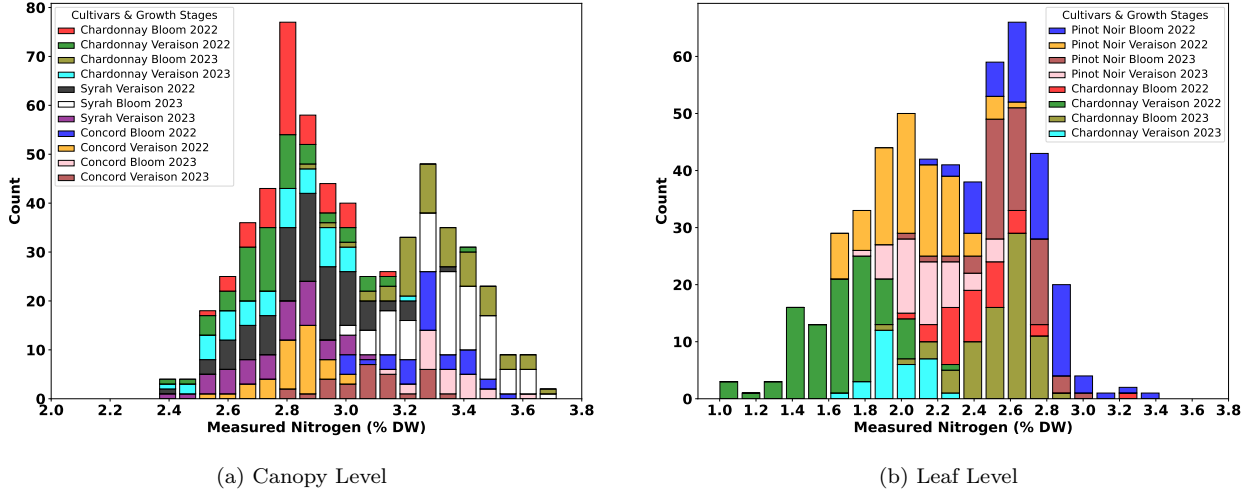


Figure 3: Distribution of measured nitrogen concentration in grapevine leaves. (a) Canopy level; (b) Leaf level.

attributed to the sampling method at the canopy level, which involves collecting multiple leaves from different parts of the vine, capturing a broader picture of the overall N concentration of the vine. This method removes individual leaf level variability caused by localized environmental factors, such as shading or exposure to sunlight. Additionally, looking at just the Chardonnay data, it is also likely that the Oregon vineyards had overall lower N status than the Washington vineyards shown in Figure 3. Furthermore, each vineyard site for data collection received varying amounts of fertilizer applications. These differences in fertilization and variations in environmental conditions, soil types, and management practices between vineyards significantly influence N concentration in leaves.

3.2. Feature Selection Comparison

3.2.1. Optimum Features from Ensemble Feature Selection

The process of selecting an optimum number of features ranked by Ensemble feature selection and its impact on model performance for the canopy level and leaf level datasets is illustrated in Figure 4. The primary objective was to identify the optimal number of features at which the model’s performance either plateaus or declines. Figure 4(a) represents the results for the canopy-level dataset. In the plot, the red line denotes the RMSEs,

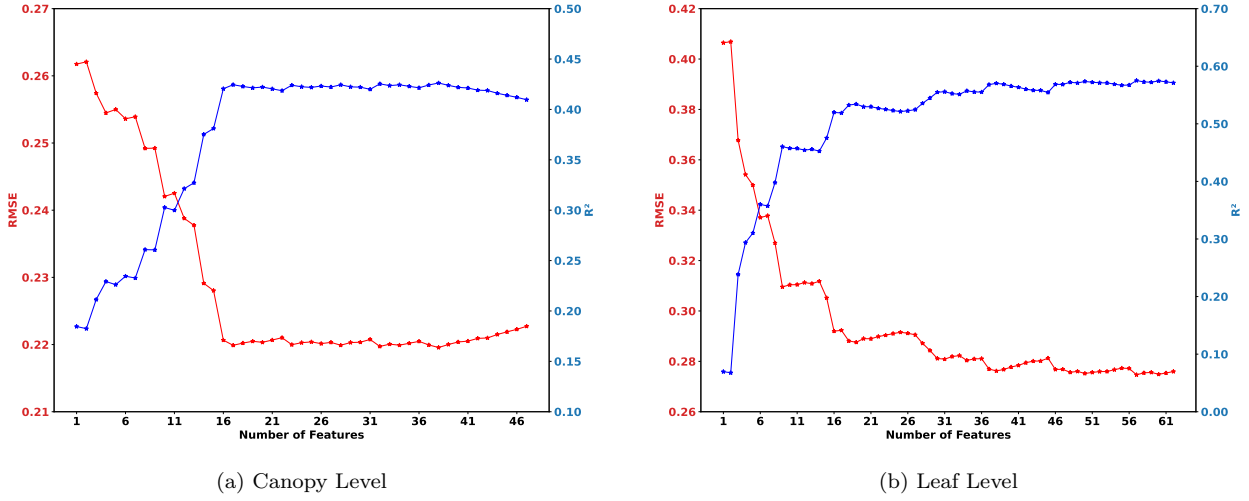


Figure 4: Change in N prediction accuracy metrics (RMSE and R^2) with increasing number of spectral features selected by the Ensemble Feature Selection method.

and the blue line represents R^2 , all plotted with an increasing number of features. Initially, the RMSE decreased as more features were added, suggesting improved model performance. However, adding more features beyond certain levels led to minimal improvement or even slight deterioration in model performance. Similarly, the R^2 values showed a rapid increase initially before plateauing around a maximum value as more features were included. This trend demonstrates that while including more features initially enhanced the model's ability to predict N concentration, the prediction ability reached a plateau beyond certain features. Figure 4(b) represents the results for the leaf-level dataset. The trends observed are consistent with the canopy-level dataset, with the model performance (e.g., R^2) increasing initially but hitting a plateau at a certain point. For the canopy-level dataset, no significant increase in model performance was observed beyond 21 features, which are identified as the significant features for predicting N concentration in grapevine leaves at the canopy level. Similarly, for the leaf-level dataset, model performance was not show significant improvement after 25 features.

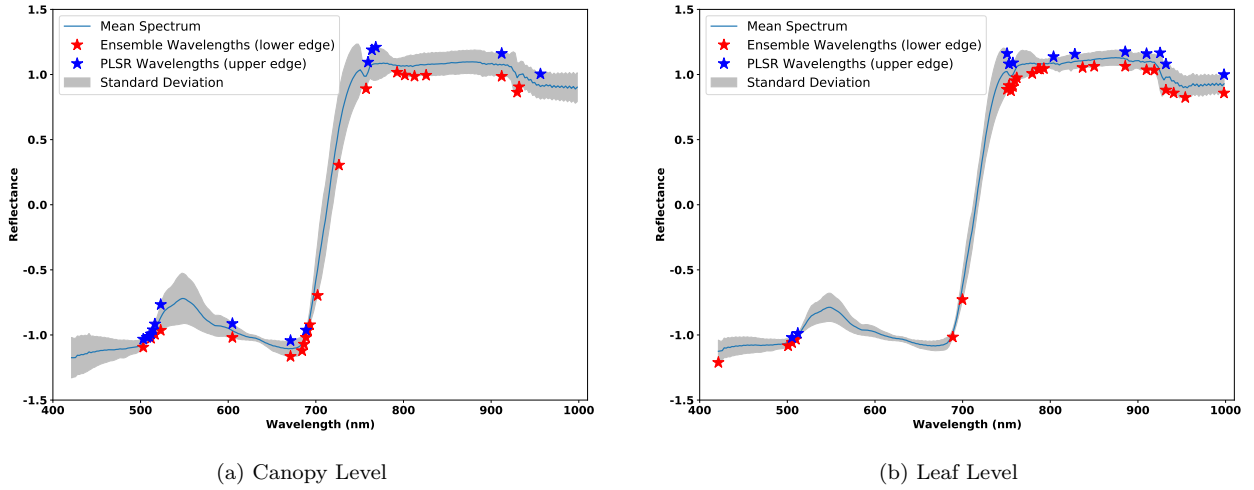


Figure 5: Mean reflectance spectrum of grapevine leaves (blue line) with standard deviation (gray shading) across the 400–1000 nm range. Red stars indicate wavelengths selected by the Ensemble feature selection method, while blue stars show those selected by PLSR. (a) Canopy level, (b) Leaf level.

3.2.2. Comparative Analysis of Feature Selection Methods

Figure 5 illustrates the selected features from the PLSR and Ensemble Feature Selection methods for the canopy- and leaf-level datasets. The mean spectrum, represented by the blue line, indicates the average reflectance pattern across all samples, with the shaded region showing the standard deviation, thus highlighting the variability at each wavelength. The blue stars on the plots denote the features selected by the PLSR method, and the red stars represent the features selected by the Ensemble Feature Selection method. Notably, there is a significant overlap between the features selected by these two methods in both leaf-level and canopy-level datasets. The common features selected by both methods are listed in Table 4, for both canopy-level and leaf-level, 8 different features were found that are common to both feature selection methods. These regions correspond to key absorption bands/features related to plant pigments and chlorophyll content, which are directly or their ratios associated with nitrogen levels (Chappelle et al., 1992; Hansen and Schjoerring, 2003; Curran, 1989). The overlapping features or bands indicate that these spectral regions are robust and reliable for predicting N concentration in grapevine leaves. The set of features or bands selected by these methods for both the canopy-level and leaf-level datasets shows that com-

binning PLSR and Ensemble Feature Selection methods effectively identifies critical spectral regions and N-predicting wavelengths. These regions have biological significance: Chlorophyll, with four N atoms in its molecular structure, plays a central role in photosynthesis, selectively absorbing blue (around 430nm) and red (around 680nm) light, while reflecting green, making plants appear green (Keller, 2020; Hennessy et al., 2020). These key wavelength regions are among those identified by our feature selection methods, highlighting their importance in detecting N levels through the chlorophyll content. Nevertheless, on average, only 1.5% of the N is in chlorophyll of light-exposed leaves; much of the remainder is bound in proteins; thus, the strong correlation between the contents of N and chlorophyll is mostly due to the complexation of chlorophyll with proteins (Evans, 1989). Researchers around the world have selected the red edge spectral bands (680-780 nm) in several studies on different crops because these wavelengths are sensitive to plant water content, as well as chlorophyll and N concentrations (Carter and Spiering, 2001). Moreover, the NIR region (above 900-970 nm) provides additional insights of water content (Sims and Gamon, 2003; Peñuelas et al., 1993) and leaf area index (LAI) (Gamon et al., 2007).

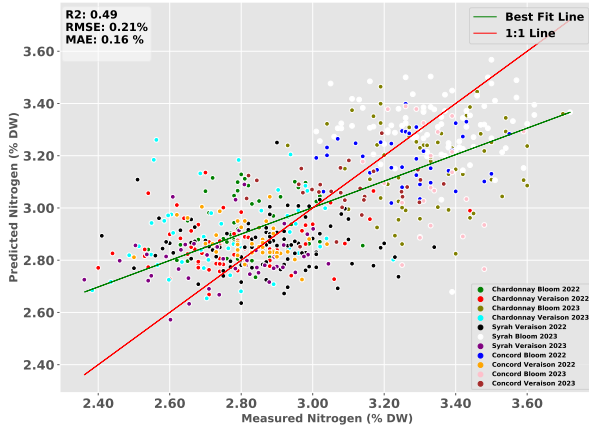
Table 4: Specific wavelengths identified by PLSR and Ensemble feature selection methods for nitrogen prediction in grapevine leaves at both leaf and canopy levels.

Level	Method	Wavelengths Selected (nm)	Count
Leaf	PLSR	505.325, 511.956, 750.674, 752.885, 757.305, 803.723, 828.037, 885.506, 909.820, 925.293, 931.924, 998.234	12
	Ensemble	421.331, 500.904, 505.325, 509.745, 688.784, 699.836, 750.674, 752.885, 755.095, 757.305, 759.516, 761.726, 779.409, 786.040, 788.250, 792.671, 836.878, 850.140, 885.506, 909.820, 918.662, 931.924, 940.765, 954.027, 998.234	25
	Common	505.325, 750.674, 752.885, 757.305, 885.506, 909.820, 931.924, 998.234	8
Canopy	PLSR	503.110, 507.530, 509.740, 511.950, 514.160, 516.370, 523.000, 604.790, 671.100, 688.780, 759.510, 763.930, 768.350, 912.030, 956.230	15
	Ensemble	503.114, 511.950, 516.370, 523.000, 604.790, 671.100, 684.360, 686.570, 688.780, 690.990, 693.200, 702.040, 726.360, 757.300, 792.670, 801.510, 812.560, 825.820, 912.030, 929.710, 931.920	21
	Common	503.114, 511.950, 516.370, 523.000, 604.790, 671.100, 688.780, 912.030	8

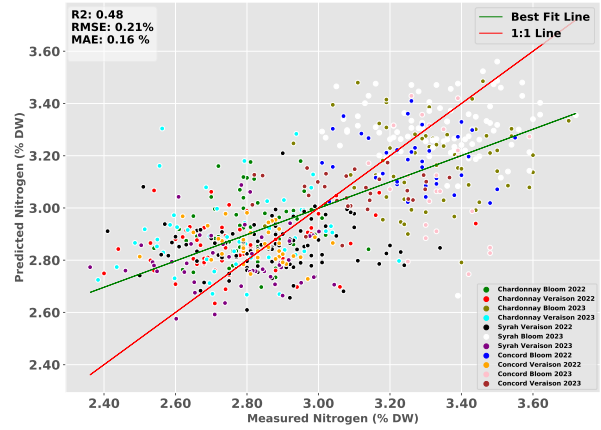
3.3. Nitrogen Prediction

3.3.1. Canopy Level Analysis

The N prediction models using Gradient Boosting and XGBoost achieved moderate predictive performance with similar accuracy metrics. The Gradient Boosting model yielded an R^2 of 0.49 (Figure 6 (a)), and the XGBoost model produced an R^2 of 0.48 (Figure 6(b)). While these R^2 values indicate that approximately half of the N variation can be explained by the models, this level of accuracy represents a meaningful advancement in field-based hyperspectral imaging for N assessment in vineyards. The plots showed that the regression line deviated from the 1:1 line, indicating slight underprediction at higher N and overpre-



(a) Canopy-level Gradient Boosting Nitrogen Estimation



(b) Canopy-level XGBoost Nitrogen Estimation

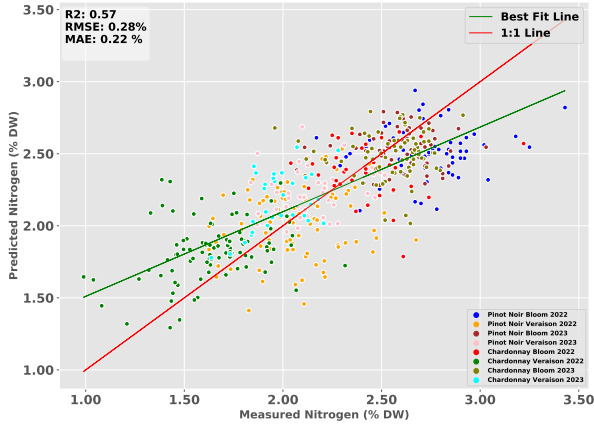
Figure 6: Model prediction performance of nitrogen concentration (% DW) at the canopy level using the 8 spectral bands selected from feature selection methods. (a) Gradient Boosting model ($R^2 = 0.49$, $RMSE = 0.21\%$, $MAE = 0.16\%$). (b) XGBoost model ($R^2 = 0.48$, $RMSE = 0.21\%$, $MAE = 0.16\%$). Data points represent measurements across three cultivars (Chardonnay, Concord, and Syrah), two phenological stages (Bloom and Veraison), and two growing seasons (2022–2023). The green line indicates the best-fit regression line, while the red line represents the ideal 1:1 relationship between predicted and measured values.

diction at lower N. This bias suggests a tendency toward the mean, likely due to limited sample representation at the extremes. The moderate prediction accuracy can be attributed to several factors. Spectral similarities arising from correlated nutrient deficiencies present a significant challenge, as most deficiencies reduce chlorophyll concentration (Rustioni et al., 2018), creating overlapping spectral signatures that mask N-specific responses (Chancia et al., 2021). Additionally, environmental variables such as lighting conditions and leaf orientation introduce variability in spectral data collection (Kang et al., 2023, 2024). Despite these challenges, the models provide valuable insights for practical N management decisions, particularly for identifying vineyard zones (e.g., areas with high or low plant N status) requiring targeted intervention rather than precise application rates. Our study strengthens the reliability of these findings by expanding beyond previous single cultivar research to include four distinct wine and juice grape cultivars across vineyards in climatically different regions (i.e., cool-humid western Oregon versus warm-arid eastern Washington) over two growing seasons and two phenological stages. The implementation of rigorous cross-

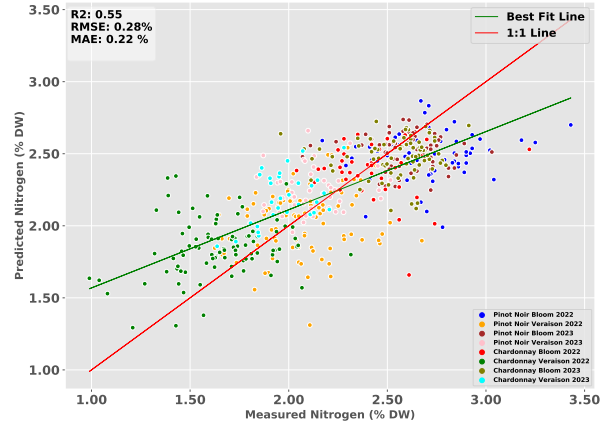
validation ensures the models' generalizability across diverse vineyard conditions, enhancing their practical applicability. The identification of eight key spectral bands creates an opportunity to develop specialized, cost-effective multispectral cameras for vineyard monitoring. Despite the moderate R^2 values, these models enable rapid, non-destructive N assessment at the canopy level, significantly reducing time, labor, and physical impact on vines compared to conventional sampling methods. Moreover, if a mobile platform with a hyperspectral camera that captures geotagged images could be readily converted to vineyard maps showing high-N and low-N zones, this would enable growers to act quickly and improve vineyard uniformity, for instance by selectively applying fertilizer N in the low-N zones only. Incorporating additional data such as soil characteristics, weather conditions, data from other stages of growth, and vine phenology into the models and exploring sensor fusion approaches that combine spectral data with other remote sensing technologies will help to achieve higher N prediction accuracy.

3.3.2. Leaf Level Analysis

The performance of the Gradient Boosting and XGBoost models in predicting N content at the individual leaf level using the selected spectral features is illustrated in Figure 7. Similar to canopy-level analysis, the models were trained using the common features (8 spectral bands, Table 4) selected by PLSR and Ensemble Feature Selection methods. For the Gradient Boosting model (Figure 7 (a)), the results show an R^2 of 0.57, and the XGBoost model (Figure 7 (b)) achieved an R^2 of 0.55. This result shows a noticeable improvement for the leaf-level predictions compared to the canopy-level predictions. This enhanced predictive performance at the leaf-level can be attributed to several factors. The wider range of N concentrations in leaf-level data provided more comprehensive training information for the models. Additionally, leaf-level spectral data significantly reduced the effects of variable leaf orientation and inconsistent sunlight exposure that typically complicate canopy-level spectral data. The more consistent light incidence at the leaf level produced spectral signatures that more closely reflected N concentration with reduced environmental noise. These advantages collectively contributed to the improved model performance, highlighting the potential



(a) Leaf-level Gradient Boosting Nitrogen Estimation



(b) Leaf-level XGBoost Nitrogen Estimation

Figure 7: Model prediction performance of nitrogen concentration (% DW) at the leaf level using the 8 spectral bands selected from feature selection methods. (a) Gradient Boosting model ($R^2 = 0.57$, $RMSE = 0.28\%$, $MAE = 0.22\%$). (b) XGBoost model ($R^2 = 0.55$, $RMSE = 0.28\%$, $MAE = 0.22\%$). Data points represent measurements across two cultivars (Pinot Noir and Chardonnay), two phenological stages (Bloom and Veraison), and two growing seasons (2022–2023). The green line indicates the best-fit regression line, while the red line represents the ideal 1:1 relationship between predicted and measured values.

of leaf-level spectral analysis for precise N status assessment. With this performance, these models can effectively identify areas with specific N requirements, enabling targeted fertilization at crucial developmental stages. While not achieving perfect predictions, they provide good accuracy to support decision-making for N management in vineyard operations.

Nitrogen concentrations in grapevine leaves measured using laboratory chemical analysis were consistently higher during the bloom stage compared to the veraison stage. This pattern was consistent in both leaf-level and canopy-level analyses across all grapevine cultivars tested (Chardonnay, Concord, Syrah, Pinot Noir), with the exception of Chardonnay in 2022, as explained in Section 3.1 and illustrated in Figure 3. This seasonal N decline aligns with findings reported in previous studies (Verdenal et al., 2021; Keller, 2020). Importantly, our prediction models successfully captured this biological trend across different datasets. This consistent pattern across multiple cultivars (grown in different vineyards) and growing seasons suggests that combining data from both bloom and veraison stages strengthens model robustness rather than developing growth-stage-specific models. While bloom-stage

measurements generally showed higher N concentrations, incorporating both stages in our predictive models provided several advantages: (1) it captured the full range of N variability throughout the growing season, (2) it increased sample size and diversity for more robust model training, and (3) it enabled the model to account for seasonal nitrogen dynamics when making predictions. Furthermore, since grapevines are significantly affected by year-to-year weather variations, incorporating data from multiple growing seasons (2022 and 2023) enhances the models' generalizability across different environmental conditions. This multi-cultivar, multi-stage, and multi-season approach led to more robust models capable of maintaining prediction accuracy despite the inherent variability in vineyard systems due to soil and climate fluctuations, making them more reliable tools for practical N management across diverse growing conditions and years.

3.4. Spectral Bands Selection Across Scales

Both PLSR and Ensemble feature selection methods showed consistency in their results, with each method identifying nearly identical spectral regions regardless of whether they were applied to leaf-level or canopy-level data, as discussed in section 3.2.2.

We further analyzed how the identified spectral bands differed between leaf-level and canopy-level as shown in Figure 8. At the leaf level, bands clustered in the blue-green (500 – 515nm), red edge (750 – 765nm), and near-infrared (850 – 940nm, 998nm) regions, which our analysis identified as responsive for N assessment in grapevine leaves. In contrast, canopy-level analysis showed somewhat different distribution patterns, with significant wavelengths concentrated in the blue-green (500 – 525nm, 604nm), red (650 – 690nm), red edge (750 – 800nm), and near-infrared (912 nm) regions. The shift toward visible spectrum bands is likely because leaf-level reflectance primarily represents direct absorption related to leaf chemistry, whereas canopy-level reflectance might be affected by additional factors such as multiple light scattering, shadowing effects, and variable leaf orientations. These canopy-level interactions shift significant spectral features toward shorter wavelengths in the visible spectrum, reflecting structural complexity inherent in remote sensing data. It was found that only two wavelength regions (500 – 525nm and 910 – 940nm) were consis-

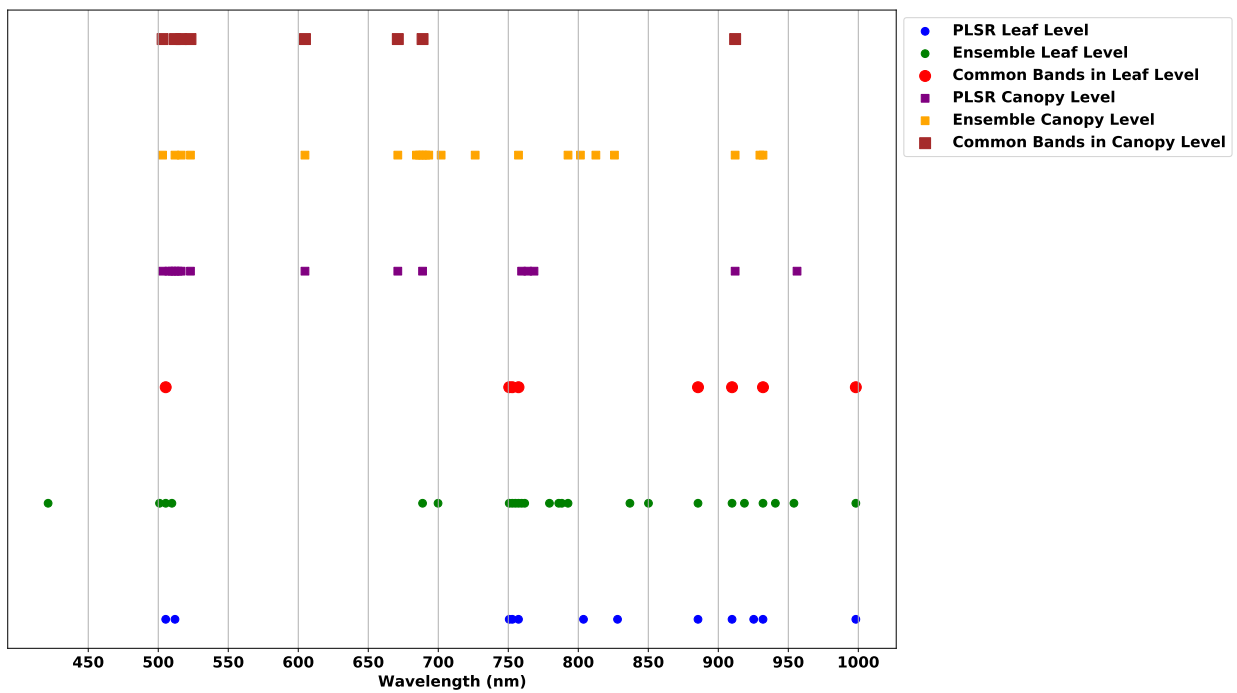


Figure 8: Spectral feature selection results for nitrogen (N) prediction in grapevine leaves, comparing PLSR (blue/purple) and Ensemble methods (green/yellow) at the leaf level (circles) and canopy level (squares). Common bands selected by both methods are shown in red (leaf level) and brown (canopy level).

tently selected across both measurement scales, suggesting these bands capture N-related physiological changes that are independent of scale complexities. These findings provide a foundation for developing specialized multispectral sensors for grapevine N assessment, with wavelengths at 500 – 525nm, 650 – 690nm, 750 – 800nm, and 900 – 950nm emerging as optimal candidates. Such targeted wavelength selection could substantially reduce sensor complexity and cost while maintaining predictive performance, advancing precision through non-destructive nitrogen monitoring technologies.

Translating these methodological findings into practical vineyard applications requires balancing the relative advantages of different measurement approaches. For N estimation modeling and feature selection, leaf-level datasets tend to be less affected by external factors than canopy-level datasets, making them advantageous for more precise model training. However, relying on just one or two leaves does not fully capture the wider variability across the vine canopies. While leaf-level data can improve prediction accuracy, a broader, canopy-level perspective is still necessary for a thorough assessment of vine’s health and to guide N management strategies (Prieto et al., 2012). While this study provides a comprehensive evaluation of feature selection and ML methods for N prediction in grapevines, there are a few areas of improvement that could be studied in the future. First, expanding the datasets to include more diverse grapevine cultivars and growing conditions/environments could enhance the generalizability of the models. Additionally, integrating spectral indices and grapevine canopy features, including canopy volume, leaf area index (LAI), and vine water potential, to account for the vine’s overall health and development status, could further improve the performance of the prediction models. Lastly, implementing these predictive models in a decision support system (DSS) for vineyard management could facilitate more precise and efficient fertilization practices to meet the needs of individual vines/plants, ultimately leading to better crop yield and quality, and resource-use efficiency.

4. Conclusion

Precise nitrogen management in vineyards impacts grape yield, quality, and vineyard sustainability, yet conventional assessment methods remain destructive, labor-intensive, and

provide limited spatial resolution. This research addressed these limitations by developing a non-invasive approach using in-field hyperspectral imaging combined with feature selection and ML models. Our robust feature selection effectively removed redundant spectral information and identified the optimal set of spectral bands from hyperspectral data for each dataset scale, which were used to assess N at the leaf-level and canopy-level. The performance of the ML models across both datasets suggested that both methods are well-suited for handling the complexity and variability inherent in hyperspectral data and identifying responsive wavelengths capable of predicting N concentration in grapevine leaves. For N concentration prediction, both XGBoost and Gradient Boosting models demonstrated similar performance across leaf-level and canopy-level. The leaf-level predictions showed higher accuracy compared to the canopy-level predictions. This work also identified key spectral regions for assessing grapevine leaf N concentration. These results showed the potential of using in-field hyperspectral imaging to monitor nitrogen levels in vineyards effectively. These results are useful for developing and implementing a viable tool for monitoring N content in individual grapevines, which is crucial for optimizing grapevine health and productivity.

Acknowledgments

This research was supported by the USDA through the National Institute of Food and Agriculture's (NIFA) Specialty Crop project award number: 2020-51181-32159. Any opinions, findings, and conclusions expressed in this publication are those of the authors and do not reflect any view from USDA or WSU. We thank Patrick A Scharf, Alan Kawakami, Syed Usama Bin Sabir, and the staff from OSU for their skilled technical assistance. Atif Bilal Asad would also like to thank Higher Education Commission(HEC) Pakistan for sponsoring his study at Washington State University.

References

Adao, T., Hruska, J., Padua, L., Bessa, J., Peres, E., Morais, R., Sousa, J.J., 2017. Hyperspectral imaging: A review on uav-based sensors, data processing and applications for agriculture and forestry. *Remote sensing* 9, 1110.

- Bioucas-Dias, J.M., Plaza, A., Camps-Valls, G., Scheunders, P., Nasrabadi, N., Chanussot, J., 2013. Hyperspectral remote sensing data analysis and future challenges. *IEEE Geoscience and Remote Sensing Magazine* 1, 6–36. doi:10.1109/MGRS.2013.2244672.
- Carter, G.A., Spiering, B.A., 2001. Leaf spectral reflectance and chlorophyll content: A multivariate analysis. *Remote Sensing of Environment* 75, 212–223.
- Chancia, R., Bates, T., Vanden Heuvel, J., van Aardt, J., 2021. Assessing grapevine nutrient status from unmanned aerial system (uas) hyperspectral imagery. *Remote Sensing* 13, 4489.
- Chappelle, E.W., Kim, M.S., McMurtrey III, J.E., 1992. Ratio analysis of reflectance spectra (rars): an algorithm for the remote estimation of the concentrations of chlorophyll a, chlorophyll b, and carotenoids in soybean leaves. *Remote sensing of environment* 39, 239–247.
- Curran, P.J., 1989. Remote sensing of foliar chemistry. *Remote sensing of environment* 30, 271–278.
- Debnath, S., Paul, M., Rahaman, D.M., Debnath, T., Zheng, L., Baby, T., Schmidtke, L.M., Rogiers, S.Y., 2021. Identifying individual nutrient deficiencies of grapevine leaves using hyperspectral imaging. *Remote Sensing* 13, 3317.
- Dong, Y., Du, B., Zhang, L., Zhang, L., 2017. Dimensionality reduction and classification of hyperspectral images using ensemble discriminative local metric learning. *IEEE Transactions on Geoscience and Remote Sensing* 55, 2509–2524.
- Evans, J.R., 1989. Photosynthesis and nitrogen relationships in leaves of c3 plants. *Oecologia* 78, 9–19.
- Fan, L., Zhao, J., Xu, X., Liang, D., Yang, G., Feng, H., Yang, H., Wang, Y., Chen, G., Wei, P., 2019. Hyperspectral-based estimation of leaf nitrogen content in corn using optimal selection of multiple spectral variables. *Sensors* 19, 2898.
- Gamon, J.A., Qiu, H.L., Sanchez-Azofeifa, A., 2007. *Ecological applications of remote sensing at multiple scales*. CRC Press.
- Gowen, A.A., O'Donnell, C.P., Cullen, P.J., Downey, G., Frias, J.M., 2007. Hyperspectral imaging—an emerging process analytical tool for food quality and safety control. *Trends in food science & technology* 18, 590–598.
- Hansen, P., Schjoerring, J., 2003. Reflectance measurement of canopy biomass and nitrogen status in wheat crops using normalized difference vegetation indices and partial least squares regression. *Remote sensing of environment* 86, 542–553.
- Hennessy, D., et al., 2020. Hyperspectral imaging for plant disease detection and plant phenotyping. *Trends in Plant Science* 25, 1000–1016.
- Jaynes, D., Colvin, T., Karlen, D., Cambardella, C., Meek, D., 2001. Nitrate loss in subsurface drainage as affected by nitrogen fertilizer rate. *Journal of environmental quality* 30, 1305–1314.
- Kalacska, M., Lalonde, M., Moore, T., 2015. Estimation of foliar chlorophyll and nitrogen content in an

- ombrotrophic bog from hyperspectral data: Scaling from leaf to image. *Remote Sensing of Environment* 169, 270–279.
- Kang, C., Diverres, G., Achyut, P., Karkee, M., Zhang, Q., Keller, M., 2023. Estimating soil and grapevine water status using ground based hyperspectral imaging under diffused lighting conditions: Addressing the effect of lighting variability in vineyards. *Computers and Electronics in Agriculture* 212, 108175.
- Kang, C., Diverres, G., Karkee, M., Zhang, Q., Keller, M., 2024. Assessing grapevine water status through fusion of hyperspectral imaging and 3d point clouds. *Computers and Electronics in Agriculture* 226, 109488.
- Keller, M., 2020. *The Science of Grapevines*. 3 ed., Elsevier Academic Press, London, UK.
- Keller, M., Hrazdina, G., 1998. Interaction of nitrogen availability during bloom and light intensity during veraison. ii. effects on anthocyanin and phenolic development during grape ripening. *American Journal of Enology and Viticulture* 49, 341–349.
- Liu, L., Ji, M., Buchroithner, M., 2017. Combining partial least squares and the gradient-boosting method for soil property retrieval using visible near-infrared shortwave infrared spectra. *Remote Sensing* 9, 1299.
- Liu, N., Townsend, P.A., Naber, M.R., Bethke, P.C., Hills, W.B., Wang, Y., 2021. Hyperspectral imagery to monitor crop nutrient status within and across growing seasons. *Remote Sensing of Environment* 255, 112303.
- Lyu, H., Grafton, M., Ramilan, T., Irwin, M., Sandoval, E., 2023. Assessing the leaf blade nutrient status of pinot noir using hyperspectral reflectance and machine learning models. *Remote Sensing* 15, 1497.
- Ma, W., Gong, C., Hu, Y., Meng, P., Xu, F., 2013. The hughes phenomenon in hyperspectral classification based on the ground spectrum of grasslands in the region around qinghai lake, in: *International Symposium on Photoelectronic Detection and Imaging 2013: Imaging Spectrometer Technologies and Applications*, SPIE. pp. 363–373.
- Mehmood, T., Liland, K.H., Snipen, L., Sæbø, S., 2012. A review of variable selection methods in partial least squares regression. *Chemometrics and Intelligent Laboratory Systems* 118, 62–69. URL: <https://www.sciencedirect.com/science/article/pii/S0169743912001542>, doi:<https://doi.org/10.1016/j.chemolab.2012.07.010>.
- Moghimi, A., Yang, C., Marchetto, P.M., 2018. Ensemble feature selection for plant phenotyping: a journey from hyperspectral to multispectral imaging. *IEEE Access* 6, 56870–56884.
- Omidi, R., Moghimi, A., Pourreza, A., El-Hadedy, M., Eddin, A.S., 2020. Ensemble hyperspectral band selection for detecting nitrogen status in grape leaves, in: *2020 19th IEEE International Conference on Machine Learning and Applications (ICMLA)*, pp. 286–293.
- Paudel, A., Brown, J., Upadhyaya, P., Asad, A.B., Kshetri, S., Davidson, J.R., Grimm, C., Thompson, A., Sallato, B., Whiting, M.D., et al., 2025. Machine vision-based assessment of fall color changes in apple

- leaves and its relationship with nitrogen concentration. *Computers and Electronics in Agriculture* 236, 110366.
- Peanusaha, S., Pourreza, A., Kamiya, Y., Fidelibus, M.W., Chakraborty, M., 2024. Nitrogen retrieval in grapevine (*vitis vinifera* l.) leaves by hyperspectral sensing. *Remote Sensing of Environment* 302, 113966.
- Peng, X., Chen, D., Zhou, Z., Zhang, Z., Xu, C., Zha, Q., Wang, F., Hu, X., 2022. Prediction of the nitrogen, phosphorus and potassium contents in grape leaves at different growth stages based on uav multispectral remote sensing. *Remote Sensing* 14, 2659.
- Peñuelas, J., Filella, I., Biel, C., Serrano, L., Save, R., 1993. The reflectance at the 950–970 nm region as an indicator of plant water status. *International journal of remote sensing* 14, 1887–1905.
- Prieto, J.A., Louarn, G., Perez Pena, J., Ojeda, H., Simonneau, T., Lebon, E., 2012. A leaf gas exchange model that accounts for intra-canopy variability by considering leaf nitrogen content and local acclimation to radiation in grapevine (*vitis vinifera* l.). *Plant, cell & environment* 35, 1313–1328.
- Pullanagari, R., Kereszturi, G., Yule, I., 2016. Mapping of macro and micro nutrients of mixed pastures using airborne aisafenix hyperspectral imagery. *ISPRS Journal of Photogrammetry and Remote Sensing* 117, 1–10.
- Rivera-Caicedo, J.P., Verrelst, J., Muñoz-Marí, J., Camps-Valls, G., Moreno, J., 2017. Hyperspectral dimensionality reduction for biophysical variable statistical retrieval. *ISPRS journal of photogrammetry and remote sensing* 132, 88–101.
- Robinson, J.B., 2005. Critical plant tissue values and application of nutritional standards for practical use in vineyards.. *American Society for Enology and Viticulture, Davis*. p. 61–68.
- Rustioni, L., Grossi, D., Brancadoro, L., Failla, O., 2018. Iron, magnesium, nitrogen and potassium deficiency symptom discrimination by reflectance spectroscopy in grapevine leaves. *Scientia Horticulturae* 241, 152–159.
- Schreiner, R.P., Lee, J., Skinkis, P.A., 2013. N, p, and k supply to pinot noir grapevines: Impact on vine nutrient status, growth, physiology, and yield. *American Journal of Enology and Viticulture* 64, 26–38.
- Sharma, S., Batra, N., et al., 2019. Comparative study of single linkage, complete linkage, and ward method of agglomerative clustering, in: 2019 international conference on machine learning, big data, cloud and parallel computing (COMITCon), IEEE. pp. 568–573.
- Sims, D.A., Gamon, J.A., 2003. Estimation of vegetation water content and photosynthetic tissue area from spectral reflectance: a comparison of indices based on liquid water and chlorophyll absorption features. *Remote sensing of environment* 84, 526–537.
- Smart, R., 1991. Canopy microclimate implications for nitrogen effects on yield and quality, in: *Proceedings of the International Symposium on Nitrogen in Grapes and Wine: Seattle, Washington, Usa 18-19 june 1991*, American Society for Enology and Viticulture, ASEV. pp. 90–101.

- Thomidis, T., Zioziou, E., Koundouras, S., Karagiannidis, C., Navrozidis, I., Nikolaou, N., 2016. Effects of nitrogen and irrigation on the quality of grapes and the susceptibility to botrytis bunch rot. *Scientia Horticulturae* 212, 60–68.
- USDA, NASS, 2024. Press release. URL: https://www.nass.usda.gov/Statistics_by_State/Idaho/Publications/Census_Press_Releases/2024/FRUIT.pdf.
- Verdenal, T., Dienes-Nagy, Á., Spangenberg, J., Zufferey, V., Spring, J.L., Viret, O., Marin-Carbonne, J., Van Leeuwen, C., 2021. Understanding and managing nitrogen nutrition in grapevine: A review. *Oeno one* 55.
- Vigneau, N., Ecartot, M., Rabatel, G., Roumet, P., 2011. Potential of field hyperspectral imaging as a non destructive method to assess leaf nitrogen content in wheat. *Field Crops Research* 122, 25–31.
- Xu, X.g., Zhao, C.j., Wang, J.h., Zhang, J.c., Song, X.y., 2014. Using optimal combination method and in situ hyperspectral measurements to estimate leaf nitrogen concentration in barley. *Precision Agriculture* 15, 227–240.
- Yao, X., Huang, Y., Shang, G., Zhou, C., Cheng, T., Tian, Y., Cao, W., Zhu, Y., 2015. Evaluation of six algorithms to monitor wheat leaf nitrogen concentration. *Remote Sensing* 7, 14939–14966.
- Zou, X., Wang, Q., Chen, Y., Wang, J., Xu, S., Zhu, Z., Yan, C., Shan, P., Wang, S., Fu, Y., 2025. Fusion of convolutional neural network with xgboost feature extraction for predicting multi-constituents in corn using near infrared spectroscopy. *Food Chemistry* 463, 141053.